Robust high content assessment of heterogeneous drug effects in 3D microenvironments

Vasanth S. Murali[1,2], Bo-Jui Chang[1], Reto Fiolka[1], Gaudenz Danuser[1,2], Murat Can Cobanoglu[2], Erik S. Welf[1,2,*]

[1]Department of Cell Biology, UT Southwestern Medical Center, Dallas, TX

[2]Lyda Hill Department of Bioinformatics, UT Southwestern Medical Center, Dallas, TX

*Corresponding author; email: erik.welf@utsouthwestern.edu

Abstract

Compared to time consuming and costly *in vivo* experiments on drug effects at single cell level, *in vitro* conditions offer increased throughput for evaluating molecular interventions in a controlled context. However, our growing appreciation for the role of the extracellular microenvironment in cellular homeostasis calls into question whether typical cell culture conditions can reflect the outcome of interventions *in vivo*. As a result *in vitro* assays have been developed to incorporate more complex microenvironmental parameters, but at the cost of increasing experimental complexity. Optimization of measurement and experimental parameters is necessary to maximize the throughput and precision of these more complex experiments. Here we develop a methodology to quantify proliferation and viability of single cells in 3D culture conditions, leveraging automated microscopy and image analysis to facilitate reliable and high-throughput measurements. The single cell resolution of this approach enables stratification of heterogeneous populations of cells into differentially responsive subtypes, and we detail experimental conditions that can be adjusted to increase either throughput or robustness of the assay. Specifically we evaluate the effect of treatment time, sample volume, and cell fate detection methods, including flow cytometry, wide field fluorescence microscopy, and light sheet fluorescence microscopy. Applying this approach to a test case, we evaluate the effectiveness of a combination of RAF and MEK inhibitors on melanoma cells, we show that cells cultured in 3D collagen-based matrices are more sensitive than cells grown in 2D culture, and that cell proliferation is much more sensitive than cell viability. Surprisingly, we find that cells grown in 3D cultured spheroids exhibit equivalent sensitivity to single cells grown in 3D collagen, suggesting that for the case of melanoma, a 3D single cell model may be equally effective as 3D spheroids models. We also illustrate the importance of measuring cell fates at the single cell by showing heterogeneity in cell responses to drug treatment. Furthermore, we show that spheroids grown from single cells exhibit dramatic heterogeneity in drug response, suggesting a heritable drug resistance can arise stochastically in single cells but be retained by subsequent generations. In summary, image-based analysis renders cell fate detection robust, sensitive, and high-throughput, enabling cell fate evaluation of single cells in more complex and realistic microenvironmental conditions.

Introduction:

3D models to interrogate the role of the physiological microenvironment in cell fate

A fundamental paradigm in cell biological studies involves evaluation of cell responses to molecular perturbations. These perturbations typically leverage gene disruptions or pharmaceutical intervention to affect protein abundance or activity. Often, the responses to such perturbations are measured on cells subjected to *in vitro* conditions under the assumption that the observed phenotypes would translate to similar phenotypes *in vivo*. However emerging evidence suggests that the three-dimensional characteristics of the cell microenvironment, including matrix dimensionality and stiffness, in part determine what phenotype will result from a certain perturbation (Leight, et al., 2017; Paszek, et al., 2005; Wells, 2008). As a result, cell biology researchers are increasingly turning towards more complex three-dimensional assays to study cells in culture. Especially for pharmaceutical candidate screening, these assays are often considered too complex, expensive, or difficult to implement (Edmondson, et al., 2014; LaBarbera, et al., 2012; Santo, et al., 2017). Unfortunately, this conclusion leads to a lack of data elucidating how perturbations affect cells under more complex conditions. Therefore, it is critical that we design assays that facilitate high-throughput evaluation of molecular perturbation under more complex microenvironmental conditions, and generate data describing the role of the microenvironment in determining how cells respond to perturbation.

Single cell resolution measurements of cell fate

In addition to ignoring the role of the microenvironment in drug screening studies, many high-throughput assays neglect the effect of cell heterogeneity despite observations of drug resistance due to inherent or acquired heterogeneity in drug response (Comin, et al., 2017; Shaffer, et al., 2017; Su, et al., 2017; Tirosh, et al., 2016). For example, the difference between a compound that reduces proliferation in 100% of cells and a compound that kills 50% of cells, while leaving proliferation unaffected in the remaining cells, may result in dramatic clinical differences. Unfortunately most drug screening assays employing measurements such as cell luminescence or enzymatic conversion activity as proxy measurements for cell number cannot discriminate between these situations (Santo, et al., 2017). Such measurements can yield imprecise results because reduced activity can mean there are fewer cells due to either decreased cell proliferation, increased cell death, or reduced cellular/metabolic activity. In order to evaluate drugs targeted for a specific purpose, assays must be capable of distinguishing these three effects in single cells, with the ultimate goal of integrating this capability into a high-throughput assay that is capable of discerning alternative cell fates at single cell resolution.

A high-throughput, single cell imaging based assay to measure cell fates in complex 3D samples

With the present work, we demonstrate the implementation of a simple, inexpensive method for quantifying cell fates in response to drug treatment. We show the importance of matrix dimensionality and mechanics of the cell microenvironment by comparing melanoma cell responses under different experimental conditions during treatment with RAF/MEK inhibitor combination (RMIC) (Long, et al., 2017). Our imaging-based assay can achieve relatively high throughput while maintaining single-cell resolution using automated microscopy and image analysis. Furthermore, we show that cytostatic and cytotoxic effects occur at different drug concentrations. We also show that the approach is amenable to evaluation of drug effects on a spheroid model. Surprisingly, we find that cells grown in spheroids exhibit

very similar drug responses to single cells in a 3D microenvironment, in contrast to cells grown on 2D plastic plates. Therefore, we conclude that, at least under the conditions evaluated here, single cells in 3D microenvironments may be substituted for spheroid models of melanoma in order to dramatically increase assay throughput.

Materials and Methods:

Tissue culture materials

A375 melanoma cells harboring the BRaf V600E mutatio were purchased from ATCC (CRL-1619). DMEM with high glucose and L-glutamine was purchased from Gibco (11965-167). A375 cells were cultured in DMEM supplemented with 10% fetal bovine serum (FBS). Two patient derived xenograft (PDX) cell models PDX1 and PDX2 were acquired from the University of Michigan via Sean Morrison at UT Southwestern Medical Center. PDX1, like A375, is a BRaf V600E mutant melanoma cell line and PDX2 is a BRaf wild type (WT) melanoma cell line. Both PDX1 and PDX2 primary cells were cultured in Dermal Basal Medium purchased from ATCC (PCS-200-030), supplemented with adult melanocyte growth kit purchased from ATCC (PCS-200-042), which includes rh insulin, ascorbic acid, L-Glutamine, epinephrine, $CaCl_2$, peptide growth factor and M8 supplement. Trypsin/EDTA was purchased from Thermo Fisher (R001100). For 3D culture, collagen I was purchased from Advanced Biomatrix (5005-100). Dabrafenib (Dab), a BRaf V600-targeting inhibitor (GSK2118436), and Trametinib (Tram), a potent MEK1/2 inhibitor (GSK1120212) were purchased from Selleckchem. Ethidium homodimer, a cell impermeant viability marker, was purchased from molecular probes (E1169). Apopxin, a phosphatidylserine sensor, was purchased from ABCAM (ab176749). Hoechst 33342 nuclear stain was purchased from molecular probes (H3570). Click-iT based imaging kit (C10340) and flow cytometry kit (C10632) were purchased from molecular probes. Phenol red free DMEM with high glucose and L-glutamine for fluorescence imaging was purchased from Gibco (21063-045). The phenol red free media was supplemented with 10% FBS. Hanks balanced salt solution (HBSS) with no calcium or magnesium was purchased from Gibco (14170112). Collagenase Type I powder to breakdown collagen was purchased from Gibco (17100017). Tetrafluoroethylene perfluoropropylene (FEP) tubes for spheroid light sheet imaging were purchased from BOLA, Germany (1815-04).

2D cell culture

All 2D cell cultures were performed in 24 or 96 well plates. Cells at ~70% confluency were washed in 1X PBS, trypsinized, and harvested at 500 g for 5 min. The cell pellet was then resuspended in 1-5 mL media depending on the cell density. The concentration of cells was determined using a cell counter and the dilution was adjusted to 200µL per well for 96 well and 500µL per well for 24 well plates. The cells were seeded at a final density of 15,000 cells/well for 24 well and 5,000 cells/well for 96 well plates. The cells were incubated overnight to allow them to attach to the bottom of the dish. For drug evaluation in 2D, a 10mM stock drug concentration was prepared in DMSO. A 2X desired concentration of the drug was first prepared in media. This was followed by a 1:1 dilution in media, which yielded the desired final concentration. Controls received the same amount of vehicle (DMSO) as the drug treated cells. The cells with drug were then incubated for the desired time, and 24h prior to analyzing the results EDU was added. A 20µM EDU solution was mixed with 2X drug and diluted 1:1 with media to give a final concentration of 10µM EDU and was incubated with the cells for 24h.

3D cultured single cell culture and spheroids

All 3D cell culture experiments were performed in 24 or 96 well plates. 10X PBS, 1M NaOH and water were pre-warmed in a 37°C water-bath. The multi well plate was pre-warmed in 37°C incubator and an aliquot of 3mg/mL collagen was brought to room temperature. Cold reagents can lengthen the collagen polymerization time, resulting in cell settling at the bottom of the dish, which does not recapitulate the 3D morphology. Cells at ~70% confluency were washed in 1X PBS, trypsinized, and harvested at 500 g for 5 min. The cell pellet was then resuspended in 1-5 mL media depending on the cell density. The concentration of cells was determined using a cell counter and the desired volume of cells were centrifuged to acquire a pellet with the desired cell number. The pellet was resuspended in 2mg/mL collagen. To prepare collagen at a final concentration of 2mg/mL from 3.2mg/mL stock, we combined 100µL 10X PBS, 10µL 1M NaOH, 250µL water and 640µL of 3.1 mg/mL collagen stock. The pH was measured to be between 7-7.4 using pH strips. The cell pellet was resuspended in 2mg/mL collagen and added to the pre-warmed multi-well plate. The cells were incubated for 30 min in 37°C incubator. Collagen polymerization was observed through change in color of the solution from a transparent solution to an cloudy gel. Media was then added to cells and incubated overnight. For RMIC evaluation in 3D, drug dilution was performed as described above for 2D cell culture.

A375 melanoma cells did not form robust spheroids by either the hanging drop method or by culturing cells in low adhesions dishes. Therefore, spheroids were created in 3D collagen by suspending single cells in collagen and culturing them over 10 days with frequent replacement of media to form 3D cultured spheroids.

RMIC treatment as a function of concentration in 2D and 3D

A375, PDX1 and PDX2 melanoma cells were setup in multi-well plates in 3D collagen and 2D culture platforms. To determine the effect of concentration in 3D and 2D cell culture platforms, the cells were incubated with RMIC at 10nM Dab+1nM Tram, 100nM Dab+10nM Tram and 1µM Dab+100nM Tram with a DMSO control. The DMSO and RMIC treated cells were incubated for 3 days as a function of concentration. Forty-eight hours post incubation with RMIC, 10µM EDU was added to cells along with the desired DMSO and RMIC concentration and cells were incubated for an additional 24h for a total of 3 days incubation with RMIC.

RMIC treatment as a function of time in 2D and 3D

A375 cells were setup in multi-well plates in 3D collagen and 2D. To determine the effect of incubation time, 3D and 2D cell culture platforms were incubated with RMIC at a concentration of 1µM Dab+100nM Tram. The drug was incubated for 3, 2 and 1 days with corresponding DMSO controls. 10µM EDU was added to all the samples 24h prior to analysis.

Viability imaging in 2D and 3D

Following treatment with RMIC, the cells were tested for viability as a function of concentration and time. The drug treated media was aspirated from the cells and incubated with 4µM ethidium homodimer, 2µL Apopxin per 100µL media and 15µg/mL Hoechst 33342 in phenol red free medium supplemented with 10% FBS. The cells were incubated with fluorescent reagents for 30 min. Following incubation, imaging was performed with a Nikon *Ti* epifluorescence microscope with an OKO temperature and CO_2 control system regulated at 37°C with 5% CO_2. The cells in 3D were imaged with a z-step size of 2.5µM and a total

of 201 steps. Following image acquisition, the cells were prepared for Click-iT EDU imaging to determine cell proliferation.

Proliferation imaging with Click-iT EDU in 2D and 3D

Following viability imaging, the cells in 2D and 3D after viability imaging were washed with 1X PBS. Following washing, the cells cultured in 3D were fixed with 4% paraformaldehyde for 30 min at 37°C, and the cells in 2D were fixed for 20 min at room temperature. The fixed cells were permeabilized with 0.5% Triton X-100 for 30 min in 3D and 20 min in 2D. Note that the 0.5% Triton X-100 was prepared from a 25% stock solution. The 25% stock should be stored at 4°C and diluted to 0.5% before use. The Click-iT reaction was then performed using the Click-iT EDU assay imaging kit with Alexa Fluor 647 fluorophore. The Click-iT reaction was partially modified from the manufacturer's protocol such that the Alexa Fluor 647 azide was first diluted 1:100 in DMSO before adding the amount specified by the manufacturer's protocol was then added. This dilution needs to be modified based on cell type. If the Alexa Fluor 647 is used directly as per manufacturer's protocol in 3D the dye will non-specifically bind to the collagen, creating a high background.

Image analysis using Cell Profiler and data processing

To analyze all the 2D and 3D images it was important to identify software that can be used with minimal computational experience. We identified Cell Profiler as an ideal candidate (Carpenter, et al., 2006; Kamentsky, et al., 2011) (http://cellprofiler.org). We used Cell Profiler V 2.2. To operate Cell Profiler we established image analysis pipelines that can accept our multi-point z-stack images and analyzed data for positive pixels from each channel.

The z-stack images were acquired as individual TIFF files. A distinguishing parameter such as a unique name for each channel was used while acquiring 3D and 2D images. In the input module under "NamesAndTypes" we defined the distinguishing name for each channel to help the software separate images from different channels. We used a robust background thresholding method to distinguish foreground (i.e. marked cells) and background regions. The pixel areas of foreground regions were measured for each channel.

While using two dead cell markers (apopxin and ethidium homodimer) to identify different phases of cell death, we observed some cells that were marked by both dead cell markers. To identify cells that were counted twice we created a mask to identify overlapping regions and then subtract that area so they are counted only once. For analyzing the cell proliferation data the pipeline was modified to two channels and the mask function was removed. Both the viability and proliferation data was exportedfor further quantification to a spreadsheet.

To analyze the viability data we first subtracted the overlapping pixel area of the dead cell channels (apopxin and ethidium homodimer) from the total area of the dead cells channels. A log (ratio+1) of the total pixels from hoechst to the dead cell pixels was calculated and averaged over all images acquired for a particular treatment. The average values for each treatment were normalized to the DMSO control; and these values were referred to as viability scores. Analogously, proliferation scores were computed based on averaging and normalization of the log (ratio+1) of the total pixels from Hoechst to EDU pixels.

Evaluating effect of well size by comparing viability and proliferation in 24 and 96 well plates

The effect of RMIC on viability and proliferation as a function of concentration in A375 cells was evaluated in 24 well plates. We evaluated similar experimental conditions in a 96 well plate to compare results to that of 24 well plates. A375 cells were plated in 2 mg/mL collagen in 3D. The cells were then treated with RMIC as a function of concentration for 3 days. On day 2 of RMIC treatment, 10µM EDU was added for an additional 24h. After 3 days total incubation, viability and proliferation assays were performed as described above.

Comparing imaging and flow cytometry for RMIC as a function of concentration

To validate the robustness of the 3D imaging platform, we measured RMIC effect on proliferation using the flow cytometry as an independent method. A375 cells were incubated with drugs as a function of concentration. The cells were incubated with drugs for 3 days and on day 2 of treatment, EDU at a final concentration of 10µM was added to the cells. Following incubation with RMIC and EDU, the collagen was washed with Hanks balanced salt solution (HBSS). The collagen was then treated with collagenase as per manufacturer's protocol for 30 min at 37°C to breakdown the collagen completely. Media with 10% FBS was then added to neutralize the effect of collagenase.

A flow cytometry based Click-iT reaction was performed as per manufacturer's protocol. In brief, the cells were centrifuged to collect the pellet. The pellet was resuspended in 4% PFA for fixation and permeabilized with 1X Tween-20. The Click-iT reaction was performed and the flow cytometry was gated using a negative control where the cells were not treated with EDU. To analyze the results, a uniform gating was setup by using the FlowJo software with a baseline negative control. The treated samples were the gated under the same settings.

Imaging cells in suspension using the Click-iT flow cytometry kit

Since the Click-iT EDU based imaging kit was designed for adherent cells, we aimed to design an imaging based method to determine proliferation for cells in suspension. We thus tested the application to imaging of a flow cytometry kit that is designed for suspended cells. To do so we cultured A375 melanoma cells in low adhesion 6 well plates. The cells were then treated with RMIC at 10nM Dab+1nM Tram and 1µM Dab+100nM Tram for 3 days. On day 2 of RMIC treatment, 10µM EDU was added for an additional 24h. After 3 day incubation with RMIC, Click-iT reaction was performed with the flow cytometry kit as per manufacturers protocol. The cells were also stained with Hoechst for imaging purposes. A drop of the cell suspension after the Click-iT reaction and Hoechst treatment was put on a glass slide and images were acquired on the Nikon *Ti* microscope. The cell images for nuclei Hoechst staining and EDU proliferation were analyzed on Cell Profiler.

Melanoma spheroid preparation for light sheet fluorescence microscopy (LSFM)

Tumor cell spheroids were created from single melanoma cells by culturing cells in sample holders as described here. FEP tubes were cut into small pieces with holes made along the walls using a 27G needle in order to allow media exchange across the tube. The tubes were cleaned with 30% bleach for 30 minutes and placed in 100% EtOH overnight. The sterile tubes were dried and pre-warmed in a 37°C incubator. A375 melanoma cells were prepared in 3D collagen as described above and seeded at low density within the FEP tubes. The collagen was allowed to polymerize at 37°C, fresh media was added, and then the cells were incubated for 10 days with regular replacement of media. The spheroids then underwent RMIC

treatment for 3 days with 24h EDU incubation. Following RMIC treatment and EDU incubation, the Click-iT imaging assay was performed and the spheroids were imaged on the LSFM.

To image spheroids, a low magnification LSFM was constructed with a large field of view. To increase the field of view, and improve optical penetration, a conventional dual illumination LSFM was built that permits scanning of the beam in the Z-dimension as well as pivoting the light-sheet in the sample plane to reduce shadowing and stripe artifacts (Huisken and Stainier, 2007). For illumination, four lasers (405nm, 488nm, 561nm, and 640nm, Coherent, OBIS) are combined with dichroic mirrors (MUX Series, Semrock), spatially filtered and expanded with a telescope consisting of an achromatic convex lens (f=50 mm, Thorlabs, AC254-050-A-ML), a pinhole (100 µm, Thorlabs, P100H), and an achromatic convex lens (f=400 mm, Thorlabs, AC254-400-A). An achromatic Galilean beam expander (Thorlabs, GBE02-A) further increases the laser diameter by 2x. All solid-state lasers are directly modulated with analog signals originating from a field-programmable gate array (PCIe-7252R, National Instruments) that have been conditioned with a scaling amplifier (SIM983 and SIM900, Stanford Research Systems).

For light-sheet generation, a cylindrical lens (f=50 mm, Thorlabs, ACY254-050-A) is used to focus the laser illumination into a sheet, which is relayed to the illumination objective (Nikon 10X Plan Fluorite, NA 0.3) with two mirror galvanometers (Thorlabs, GVS001), two coupling lenses (f=50 mm, Thorlabs, AC254-050-A), and a tube lens (f=200 mm, Thorlabs, ITL-200). The Z-galvanometer is conjugate to the back pupil of the illumination objective, whereas the pivot galvanometer is conjugate to the sample. To generate the second illumination arm of the microscope, a polarizing beam splitter (Newport, 10FC16PB.3) is placed after the second coupling lens, and two lenses (f=200 mm, Thorlabs, AC508-200-A) relay the scanned illumination to a second tube lens and illumination objective. Because the counter-propagating light-sheets are orthogonally polarized, there is no interference from the two light-sheets, and a half-wave plate (AHWP10M-600) placed in front of the polarizing beam splitters is used to adjust the intensity of the two light-sheets. To control the light-sheet thickness, a variable slit was placed in the back-pupil plane of the cylindrical lens, which is conjugated to the back-pupil planes of both illumination objectives.

For detection, a 16x, NA 0.8 objective lens (Nikon CFI75 LWD 16X W) and a tube lens (f=200 mm, Edmund optics, 58-520) form the image on a sCMOS camera (Hamamatsu, C11440, ORCA-Flash4.0). A laser line filter (Chroma, ZET405/488/561/640) is placed after the detection objective lens and a filter wheel (Sutter Instrument, Lambda 10-B) equipped with multiple bandpass filters is placed between the tube lens and the camera. The detection objective lens is mounted on a piezo-driven stage (Mad-City Labs, Nano-F450) that provides 450 µm travel range. The sample stage is a combination of a three-axis motorized stage (Sutter Instrument, MP285) and a rotation stage (Physik Instrumente, U-651.03). The microscope is controlled by custom-written LabVIEW software (Coleman Technologies, National Instruments).

Results:

The effect of microenvironment on drug sensitivity

Effect of RAF/MEK inhibition on proliferation and viability of 2D and 3D cell culture platforms

We first set out to determine how melanoma cells cultured in 3D collagen microenvironments reacted to RAF/MEK inhibitor combination (RMIC) compared to cells cultured on more traditional 2D polystyrene cultures plates. We chose collagen I for the scaffold since collagen I is the most abundant ECM protein in the human body (Frantz, et al., 2010; Theocharis, et al., 2016) and fills the majority of the interstitial spaces between tissues(Bosman and Stamenkovic, 2003; Mouw, et al., 2014). As such, it is commonly used as the

major scaffold in 3D cell culture assays based on natural polymers. We also chose collagen matrices in order to recreate the microenvironment melanoma cells encounter in the dermis. Compositions that more closely mimic the basement membrane would be more appropriate for cells of epithelial origin.

A375 is a readily available melanoma cell line that harbors a BRaf V600E mutation, making it an ideal model system on which to first evaluate our cell fate analysis pipeline. RMIC treatment targets the MAP kinase pathway by blocking RAF and MEK with Dab and Tram, thus inhibiting growth and proliferation. Treatment of A375 cells for three days with three different concentrations of RMIC revealed both a decrease in proliferation as well as a decrease in the fraction of viable cells, although the reduction in viability required a RMIC dose 10 times that required to elicit proliferation reduction (Figure 1). Although cells in both 3D and 2D cultures responded to RMIC, cells cultured in 3D were more sensitive to lower doses than cells cultured in 2D. These results suggest that 3D conditions may be more useful than 2D conditions for identifying lead compounds and that potentially useful compounds may have been overlooked by 2D cell culture-based screens. In addition to the increased drug sensitivity conferred by 3D culture conditions, we noted a tenfold difference in the RMIC concentration required to reduce proliferation compared to viability. We attribute the difference between viability and proliferation to direct measurement of EDU incorporation for cell proliferation, instead of general measures of cell biomass which are incapable of distinguishing between reduced proliferation and viability.

In order to determine if these results are applicable to other melanomas, we obtained melanoma cells derived from two different melanoma patients that have been maintained as PDX models (Quintana Nature 2008). The MEK inhibitor Trametinib used in our RMIC treatment, is a general MEK inhibitor and thus both PDX1 and PDX2 are expected to exhibit sensitivity. Upon measuring viability PDX1 (Figure 2A) was more sensitive to RMIC treatment than PDX2 (Figure 2C). This difference in sensitivity is associated with the treatment of Dab which targets PDX1 (BRaf V600E mutants) cells but not PDX2 (BRaf WT) cells. However, cells from both PDX models exhibited reduced proliferation under RMIC treatment and both were more sensitive to RMIC under 3D conditions compared to 2D conditions (Figure 2B & 2D). Interestingly, cells from both PDX models under 2D and 3D conditions exhibited roughly equivalent cell viability (Figure 2A & 2C), suggesting that changes to proliferation represent both a more sensitive and a more robust metric for evaluating drugs targeting the MAPK pathway in melanoma, compared to viability.

Tumor spheroid vs. single cells

Tumor spheroids are a common model for 3D cell culture, since they are believed to recapitulate *in vivo* tumor morphology (Antoni, et al., 2015; Edmondson, et al., 2014; Friedrich, et al., 2009). We sought to determine if 3D cultured spheroids yield similar results to 3D cultured single cells upon drug treatment by measuring changes to cell proliferation upon drug treatment. Spheroids were formed by seeding cells in collagen at low density and culturing for 10 days with frequent replacement of media. The spheroids were then treated with different RMIC concentrations and with a DMSO control. EDU at 10µM was added 24h prior to performing the Click-iT reaction. After a 3 day incubation with RMIC, Click-iT imaging was performed and data was analyzed using Cell Profiler. Upon normalizing with DMSO controls we observed ~7% cell proliferation at 10nM Dab+1nM Tram which was similar to the ~5% cell proliferation under similar treatment for single cells cultured in 3D (Figure 3). At concentrations of 100nM Dab+10nM Tram and 1µM Dab+100nM Tram a complete knock down in proliferation was observed both in 3D cultured spheroids and 3D cultured single cells (Figure 3). To our knowledge, this data shows for the first time a similar effect on proliferation on 3D single cells and spheroids upon RMIC treatment on a melanoma cell line. If this

result holds for all melanoma cultures and for other cancer types, it suggests that researchers may save time and money by measuring drug effects on single cells in 3D instead of culturing cells as spheroids.

Assay design parameters to tune cost, speed, and sensitivity

Effect of drug treatment time

To evaluate the effect of drug treatment time, A375 melanoma cells were treated with RMIC at 1µM Dab+100nM Tram for 1, 2 and 3 days in 2D and 3D as described in the materials and methods. We observed a reduction in viability at steady but slower rate (Figure 4A). However, reduction in proliferation was observed after a 24h incubation with a ~50% reduction in proliferation in 3D and ~10% reduction in proliferation in 2D (Figure 4B). By 48h incubation, cells cultured in both 3D and 2D showed a complete ablation of proliferation(Figure 4B). Based on the reduced time necessary to observe significant alterations in outcome, we anticipate that an efficient drug screening assay may be built upon proliferation measurement rather than cell viability. If reduced tumor cell viability is the ultimate goal of targeted melanoma therapy, then a drug targeting a different pathway may offer a more robust intervention strategy for melanoma. However, we highlight here that our assay can be used to evaluate effects to both proliferation and viability, potentially leading to more effective therapeutic discoveries targeting either proliferation or viability more efficiently than targeting both cell fates simultaneously.

Cell culture volume

Since 3D collagen adheres to the walls of the plates, and adherence to the wall might alter collagen properties sensed by the cell, which may affect how drug treatments affect cells(Han, et al., 2018; Welf, et al., 2016). Thus, we wished to understand if cells tested in 24 versus 96 well plates yielded different results. The effect of RMIC combination therapy as a function of concentration was assessed in 96 well plates where A375 cells were incubated with RMIC as a function of concentration. The cells were incubated with RMIC for 3 days following which viability and proliferation assays were performed. No significant difference was observed in the results acquired for cells in 24 and 96 well plates (Figure 4C & 4D). However greater variability was observed in the 96 well data. This may partially be attributed to the apparent stiffness associated with the collagen near the walls of the multi-well dish, which is known to affect cancer cell fates (Hirata, et al., 2015; Leight, et al., 2017). Proliferation results were similar for both the 24 and 96 well plates. Thus, either 24 well or 96 well plates may be used, giving researchers the option of leveraging the cost savings and increased throughput offered by using 96 well plates at the cost of slightly increased variability compared to larger wells.

Detection methods

Although we have focused on microscope imaging for the purpose of detecting changes to cell fate, researchers may wish to use alternative detection methods, if, for example, cells are grown in suspension or if there are concerns over the ability to image cells under different environmental conditions. Here we demonstrate that cells may be dissociated from their microenvironment and then detected using flow cytometry or imaging. Finally, we evaluate microscopy conditions to determine if the type of microscope used for imaging affects proliferation quantification.

Imaging vs. flow cytometry

To test robustness of the 3D imaging platform (Figure 5A) we validated A375 melanoma cell proliferation upon RMIC treatment using the Click-iT EDU based flow cytometry assay. The cells were treated with RMIC as a function of concentration as described in materials and methods. During the last 24 hours of RMIC treatment the cells were incubated with EDU. The collagen was then digested with collagenase as described in the materials and methods. A Click-iT reaction was performed according to the manufacturer's protocol. A negative control used for gating on the flow cytometer was created by omitting EDU from a batch of cells but subjecting them to the Click-iT reaction. The data was next analyzed using FlowJo software with uniform gating applied to treatment samples based on the negative control (Figure 5B). The results were compared to the Click-iT EDU imaging based platform (Figure 5C). Similar results were observed for both the platforms indicating the robustness of the imaging platform.

Imaging with flow cytometry reagents in suspension cells

Since the experiments performed were on adherent cells in 2D or 3D we wanted to develop an imaging based proliferation assay for non-adherent cells. To do so we setup A375 melanoma cells in low adhesion plates that were treated with RMIC as a function of concentration. Since Click-iT EDU based imaging kit was designed for adherent cells, we used the Click-iT EDU flow cytometry kit. The cells were incubated with RMIC for 3 days with EDU added on second day of treatment for 24h. The Click-iT EDU assay was performed as per manufacturer's instructions with an additional step of Hoechst staining of the nuclei. Cells in suspension were deposited on a glass slide, covered with a coverslip, and imaged (Figure 5D), then analyzed using Cell Profiler (Figure 5E). These results demonstrate the feasibility of using the flow cytometry kit along with imaging for the purpose of measuring cell fate in non-adherent cells or cells in suspension.

Epifluorescence microscopy compared to light sheet fluorescence microscopy

We aimed to test if wide-field epifluorescence microscopy is capable of measuring cell fate in complex multi-nuclear samples. To do so, we compared the results of our 3D epifluorescence imaging assays to those acquired by light sheet fluorescence microscopy (LSFM), which limits the amount of out-of-focus light from the 3D sample by exciting fluorescence only in a thin sheet. Spheroids for light sheet imaging were prepared in FEP tubes, which has a refractive index close to water thus minimizing the refraction of light. This enables a 360 degree access of the imaging objectives to the sample. Single cells in collagen were prepared in tubes and cultured for 10 days with frequent replacement of media. The spheroids were treated with RMIC for 3 days with EDU added on the second day of treatment for 24h. The Click-iT imaging assay was performed as described in the materials and methods. The light sheet images were acquired for individual spheroids with a z-step size of 1µm and analyzed in Cell Profiler (Figure 6A and 6B). Similar proliferation results were observed for 3D spheroids imaged in epifluorescence or LSFM, suggesting that imaging using commonly available epifluorescence microscopes is sufficient to quantify cell fate, even for cells in complex environments such as spheroids.

Identification of heritable drug resistance in melanoma cell spheroids

Comparing the proliferation data for 3D cultured single cells to that of spheroids from epifluorescence and light sheet images, a similar range of proliferation was observed with no statistical difference between the different modalities (Figure 7A). Further inspecting the spheroids treated with 10nM Dab+1nM Tram, we observed striking heterogeneity in proliferation: although most spheroids exhibited no proliferation, several spheroids were greatly enriched for proliferating cells (Figure 7B and 7C). Because each spheroid

was created from a single cell, this result suggests that some heritable drug resistance mechanism of the initiating cell was passed down to several generations of daughter cells, resulting in the dramatic enrichment of proliferation in some spheroids. This observation is consistent with heritable drug resistance or a phenotype switch observed in melanoma (Shaffer, et al., 2017).

Discussion

In order to streamline drug discovery, we must develop methods to evaluate compound efficacy under increasingly complex extracellular microenvironments (Macarron, et al., 2011; Workman, et al., 2017). However, experimental complexity must be balanced with throughput, cost, reproducibility, and precision. Here, we described an assay that enables high-throughput compound evaluation without sacrificing single cell resolution, readout specificity, or microenvironmental complexity. Indeed, although we evaluated this assay using 3D collagen scaffolds, it is equally amenable to other scaffolds and would be equally useful for identifying which ECM components affect drug efficacy. Our results show that even a simple 3D collagen microenvironment affects how cells respond to treatment, rendering melanoma cells more sensitive to treatment under 3D conditions compared to 2D conditions. This observation suggests that many potentially useful compounds might have been ignored because they were tested on cells under 2D conditions. The work presented here removes the barriers to measuring perturbations in more realistic microenvironments by providing a resource for sensitive, high-throughput, cost-effective compound evaluation.

In addition to facilitating study of more complex microenvironments, a key feature of the presented methodology is the ability to measure single cell responses. Conventional methods of evaluating 3D cell culture assay involve chemiluminescence or enzymatic conversion assays that yield high throughput results but at the cost of single cell resolution (Hongisto, et al., 2013; Kenny, et al., 2015). Alternatively 3D cultures may be imaged to detect responses at single cell resolution but such an approach requires complex image analysis protocols to convert high resolution images into quantitative results (Mathew, et al., 2015; Packard, et al., 2017). In this work, we employed the freely available and popular Cell Profiler image analysis package to overcome the challenges of analyzing 3D data by evaluating data through all the planes of a 3D image stack. We anticipate that the combination of automated image acquisition on a relatively low cost microscope combined with freely available analysis software will encourage application of this approach in various laboratory settings.

The ability to discriminate cytotoxic from cytostatic compounds and as a result identify more sensitive cell fate readouts will also streamline drug discovery. For example, we show that although the RAF/MEK inhibitor combination rapidly inhibits proliferation of both a melanoma cell line and two different melanoma PDX-derived cell models, it has variable effects on cell viability. These results suggest that although this treatment may be effective at slowing tumor growth, it would ultimately be more effective if combined with a more specific cytotoxic therapy. Thus, it is our hope that more sensitive, more precise measures of cell fate will enable more accurate predictions of *in vivo* efficacy that will render drug discovery and optimization more effective.

We have employed this assay to test the hypothesis that melanoma spheroids offer a more realistic paradigm for drug efficacy than 2D cultures. This is indeed the case – A375 cells grown in spheroids are more sensitive to proliferation inhibition than cells grown on plastic dishes. We observe now that cells grown individually in 3D are equally sensitive to RMIC when compared to cells grown in spheroids. This observation suggests that, if this result holds for other systems, then cells cultured in 3D collagen may be

as effective as spheroids for compound evaluation. This result would greatly reduce the time necessary to grow spheroids without sacrificing assay sensitivity, and thus would increase productivity.

Acknowledgements

This research was funded by grants from the National Institutes of Health (K25CA204526 to ESW) and the Cancer Prevention Institute of Texas to (R1225 to GD and RR160057 to RF). We would like to thank Andrew D. Jamieson for help in building Cell Profiler pipelines, Heather Grossman for cell sorting, Sean Morrison for PDX-derived cell models, Xuexia Jiang for help with file conversions and Meghan Driscoll, Etai Sapoznik for providing valuable feedback on the manuscript.

Author Contributions

V.S.M. and E.S.W. conceived the project. G.D. and M.C.C. provided intellectual input. V.S.M. made the figures. V.S.M. designed and performed the experiments. B.J.C. and R.F. constructed the LSFM. V.S.M., B.J.C., R.F., G.D., M.C.C., and E.S.W. wrote the manuscript.

Competing Interests

The authors declare no competing interests.

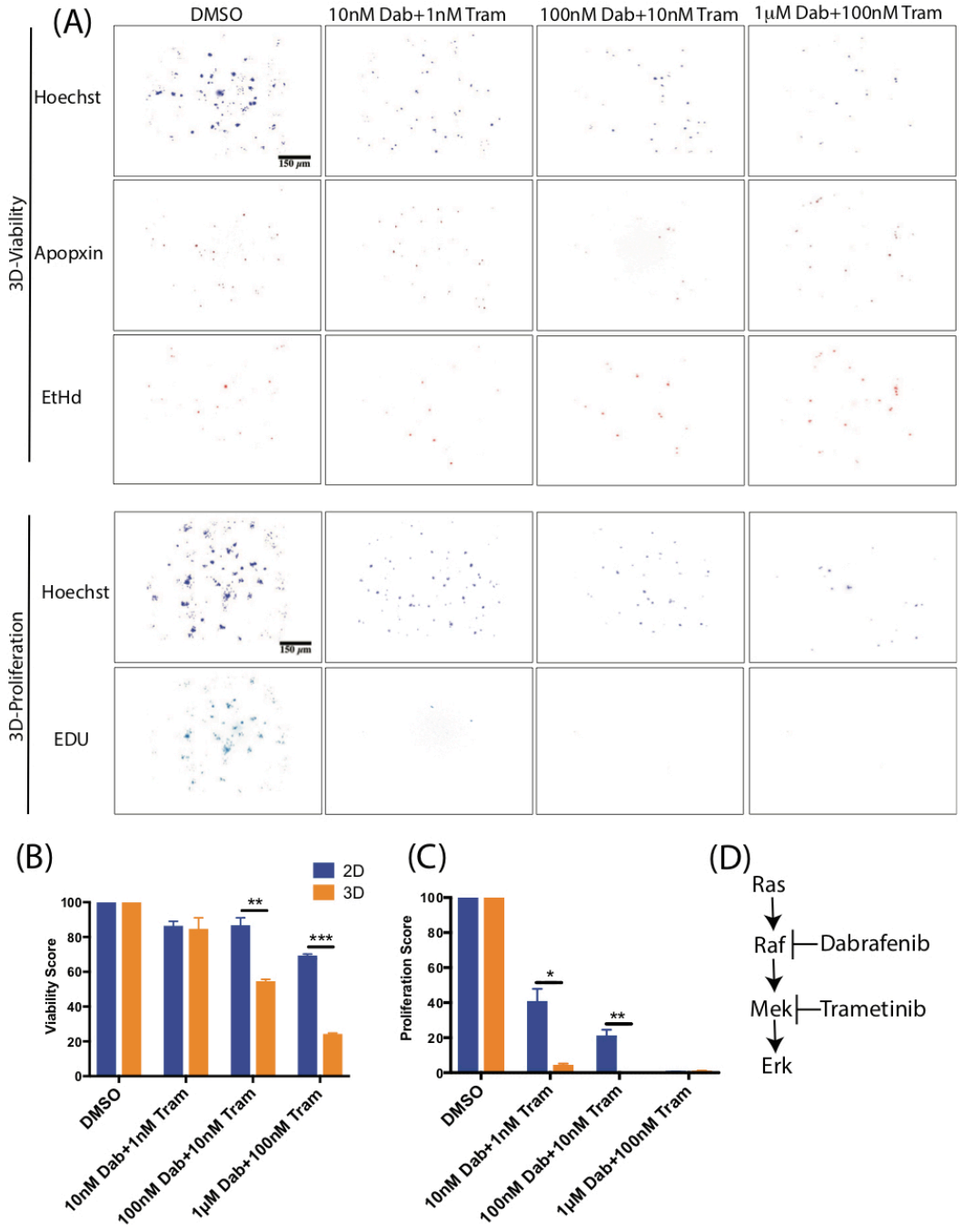

Figure 1: Evaluating RMIC treatment on A375 for viability and proliferation in 2D and 3D cell culture. A375 melanoma cells were cultured in 2D and 3D and treated with RMIC as a function of concentration. 3D Z-stack images were acquired on epifluorescence microscope with maximum intensity projections presented (A). The images were quantified using cell profiler for positive pixels for each channel. The viability score (B) and proliferation score (C) were compared for 2D and 3D cell culture systems. All data was normalized to the DMSO controls. The RMIC treatment uses Dab and Tram that block RAF and MEK in MAP kinase pathway (D).

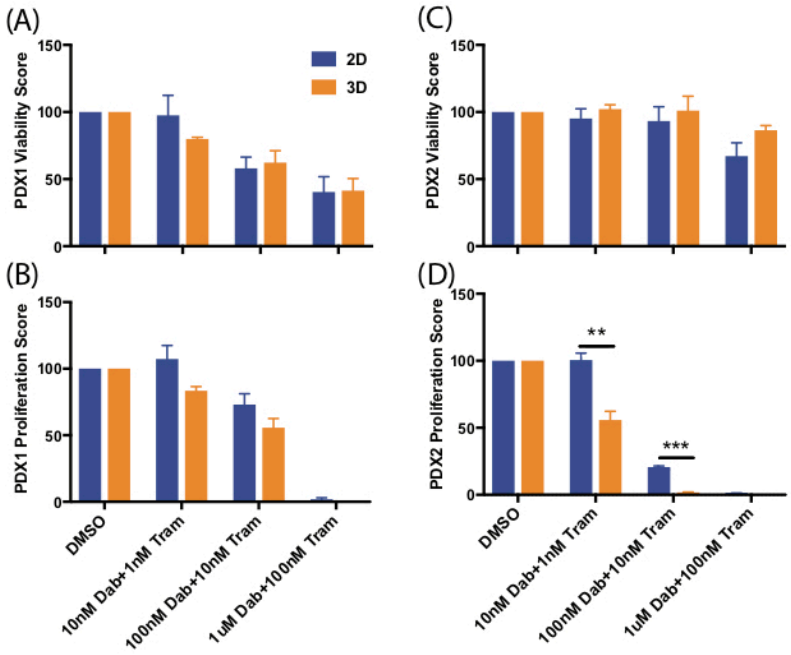

Figure 2: Evaluating RMIC treatment on PDX1 and PDX2 for viability and proliferation in 2D and 3D cell culture. PDX1, a BRaf V600E mutant melanoma cell and PDX2, a BRaf WT melanoma cell were cultured in 2D and 3D and treated with RMIC as a function of concentration. Viability and proliferation score for PDX1 (A & B) and for PDX2 (C & D) were quantified as a function of concentration and compared to 2D and 3D cell culture platforms. The data was quantified by normalizing the DMSO controls to 100% and corresponding treatments evaluated. Three independent repeats were performed with average and SEM plotted.

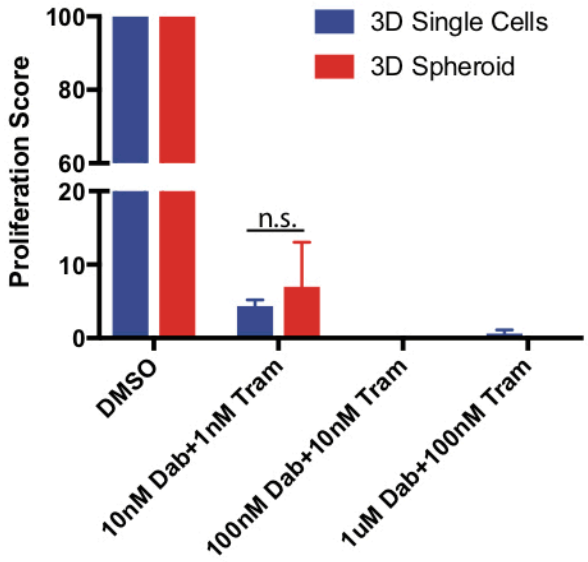

Figure 3: Effect on proliferation upon RMIC treatment on 3D cultured single cells and spheroids. A375 melanoma cells were cultured as single cells for 10 days in collagen to make 3D cultured spheroids which were treated with RMIC to evaluate the proliferation score. The data was then compared to 3D cultured single cells under similar treatment conditions. At concentration of 10nM Dab+1nM Tram similar proliferation results were observed with no statistical significance (n.s). At higher concentrations of RMIC a complete knock out in proliferation was observed in both 3D cultured single cells and spheroids thus indicating similar proliferation effects.

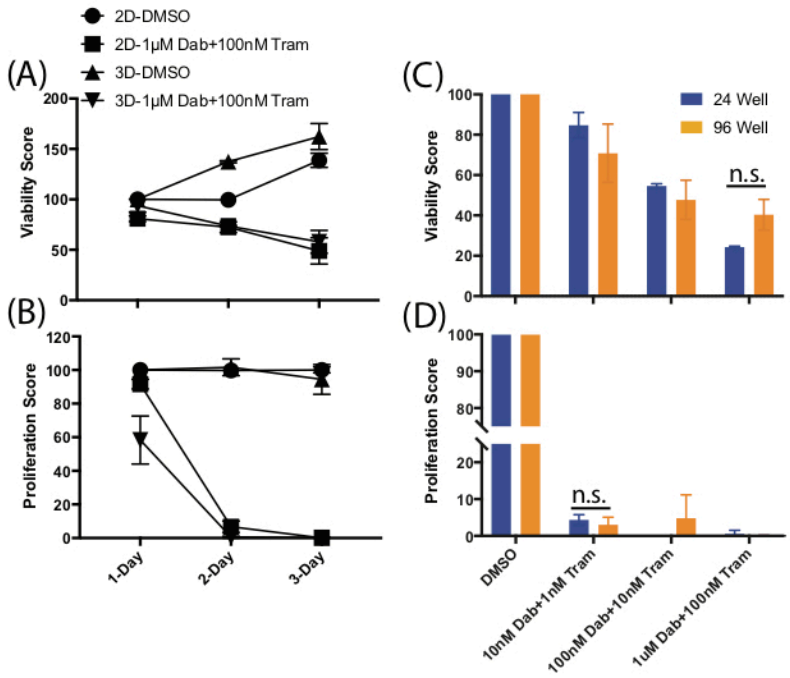

Figure 4: Assay design parameters: Incubation time and cell culture conditions. A375 melanoma cells were treated with RMIC in 2D and 3D cell cultures at 1μM Dab+100nM Tram for 1, 2, and 3 days followed by viability (A) and proliferation (B) assays. To determine effect of cell culture volumes A375 cells were cultured in 3D in 96 well plates, treated with RMIC and evaluated for viability and proliferation. The data was then compared to 24 well plates to determine effect on viability (C) and proliferation (D). No statistical significance (n.s.) was observed in comparing viability (C) and proliferation (D) between 24 and 96 well plates. The viability and proliferation scores were plotted by normalizing the DMSO control to 100%.

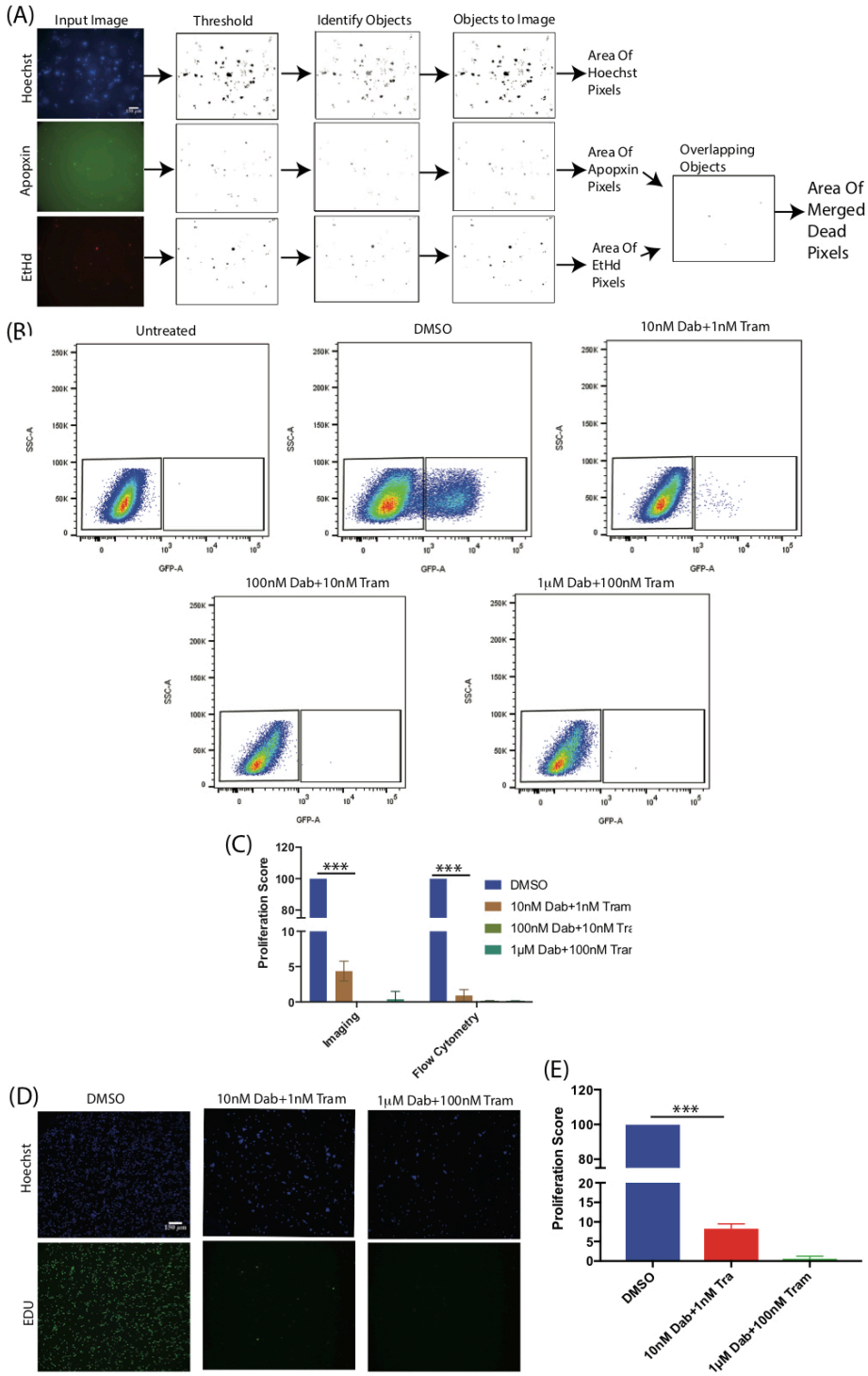

Figure 5: Detection Methods: Evaluating 3D imaging with Flow Cytometry and Imaging Suspension cells. To evaluate 3D imaging platform (A), A375 cells cultured in 3D were evaluated with flow cytometry. The cells were gated based on the negative control (B) and the results were compared to imaging platform (D). To evaluate effect of RMIC on suspension cells, A375 cells were cultured on low adhesion plates with Click-iT flow cytometry kit used. The cells were then imaged (C) and quantified using Cell Profiler (E). The proliferation scores (C & E) were plotted by normalizing to DMSO control.

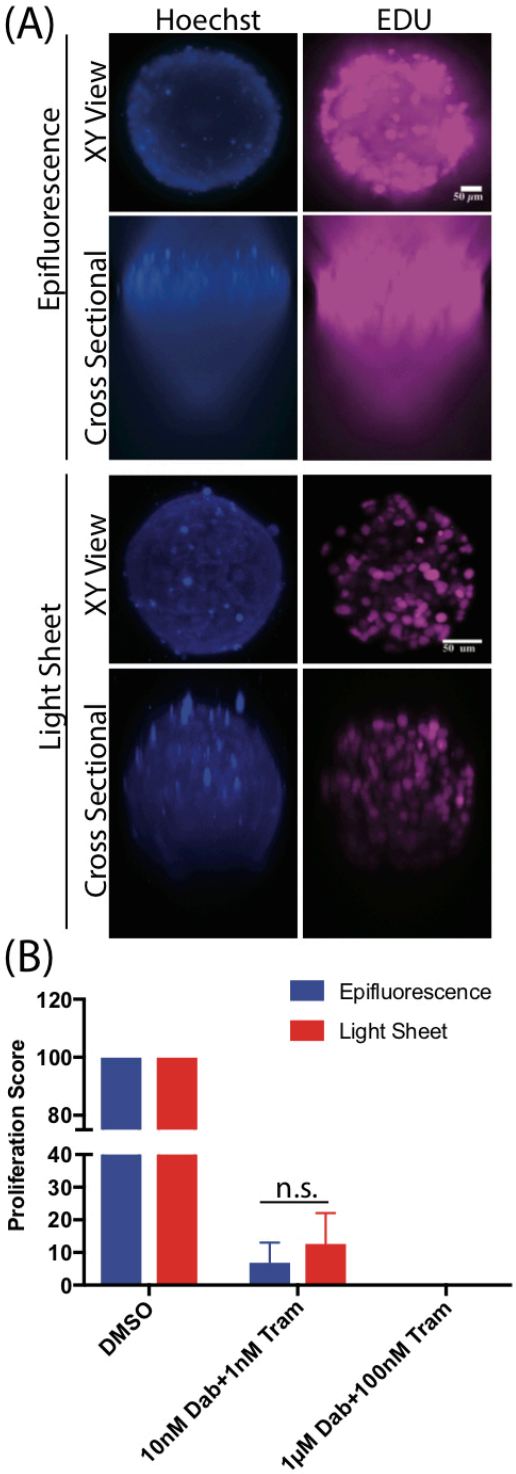

Figure 6: Evaluating epifluorescence vs light sheet spheroid imaging. A375 melanoma spheroids were prepared in collagen and treated with RMIC following which proliferation was evaluated with LSFM. The imaging was compared for the two platforms showing the XY maximum intensity projection and a cross sectional view (A). Proliferation data for spheroids from LSFM was then compared to data acquired from epifluorescence microscopy (B) with no statistical significance between the two imaging platforms. Proliferation score was quantified by normalizing to DMSO control.

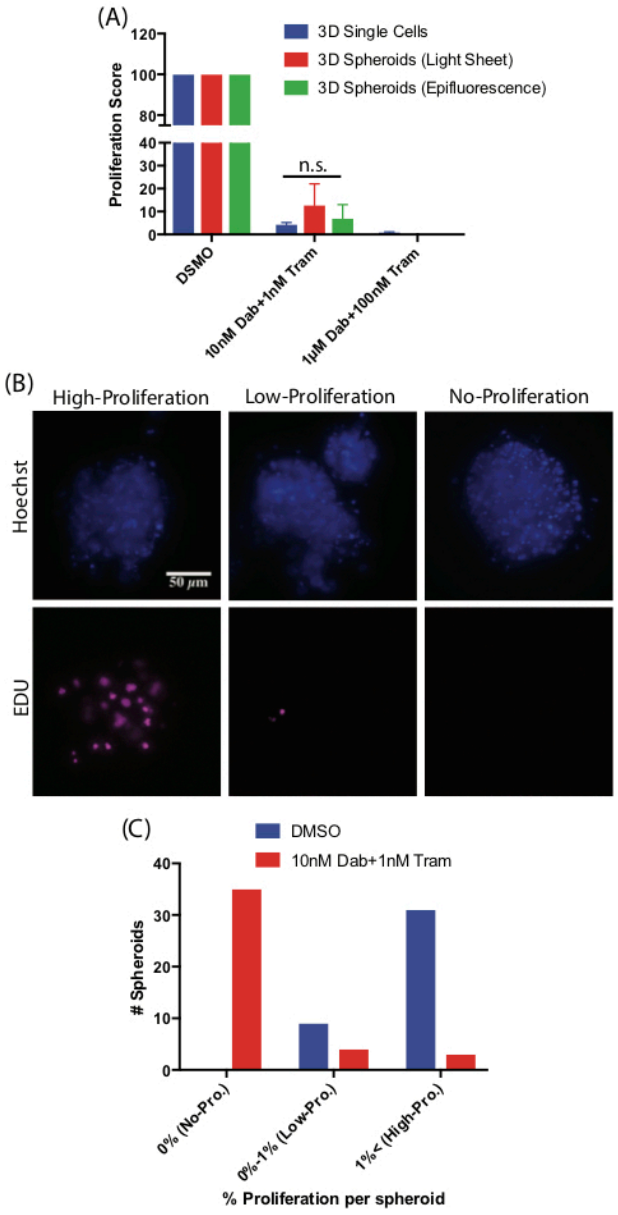

Figure 7: Clonal selection of spheroids from single cells. A375 melanoma cells were compared for proliferation upon RMIC treatment in 3D cultured single cells to that of spheroid data acquired from epifluorescence and light sheet (A). Spheroids treated with 10nM Dab+1nM Tram normalized to hoechst for individual spheroid showed a varying degree of proliferation (B). Distribution of spheroids were analyzed as high-proliferation, low-proliferation and no-proliferation (C).

Antoni, D., Burckel, H., Josset, E., and Noel, G. (2015). Three-Dimensional Cell Culture: A Breakthrough in Vivo. International Journal of Molecular Sciences 16, 5517-5527.

Bosman, F.T., and Stamenkovic, I. (2003). Preface to extracellular matrix and disease. The Journal of Pathology 200, 421-422.

Carpenter, A.E., Jones, T.R., Lamprecht, M.R., Clarke, C., Kang, I.H., Friman, O., Guertin, D.A., Chang, J.H., Lindquist, R.A., Moffat, J., et al. (2006). CellProfiler: image analysis software for identifying and quantifying cell phenotypes. Genome Biology 7, R100.

Comin, A., Thomas, G.G., Antoni, R., James R. Heath, Y.S., Wei, W., Lidia, R., Min, X., Jennifer, T., Angel, G.-D., Blanca Homet, M., et al. (2017). Single-cell analysis resolves the cell state transition and signaling dynamics associated with melanoma drug-induced resistance.

Edmondson, R., Broglie, J.J., Adcock, A.F., and Yang, L. (2014). Three-Dimensional Cell Culture Systems and Their Applications in Drug Discovery and Cell-Based Biosensors. Assay and Drug Development Technologies 12, 207-218.

Frantz, C., Stewart, K.M., and Weaver, V.M. (2010). The extracellular matrix at a glance. Journal of Cell Science 123, 4195-4200.

Friedrich, J., Seidel, C., Ebner, R., and Kunz-Schughart, L.A. (2009). Spheroid-based drug screen: considerations and practical approach. Nature Protocols 4, 309.

Hirata, E., Girotti, Maria R., Viros, A., Hooper, S., Spencer-Dene, B., Matsuda, M., Larkin, J., Marais, R., and Sahai, E. (2015). Intravital Imaging Reveals How BRAF Inhibition Generates Drug-Tolerant Microenvironments with High Integrin β1/FAK Signaling. Cancer Cell 27, 574-588.

Hongisto, V., Jernström, S., Fey, V., Mpindi, J.-P., Kleivi Sahlberg, K., Kallioniemi, O., and Perälä, M. (2013). High-Throughput 3D Screening Reveals Differences in Drug Sensitivities between Culture Models of JIMT1 Breast Cancer Cells. PLOS ONE 8, e77232.

Kamentsky, L., Jones, T.R., Fraser, A., Bray, M.-A., Logan, D.J., Madden, K.L., Ljosa, V., Rueden, C., Eliceiri, K.W., and Carpenter, A.E. (2011). Improved structure, function and compatibility for CellProfiler: modular high-throughput image analysis software. Bioinformatics 27, 1179-1180.

Kenny, H.A., Lal-Nag, M., White, E.A., Shen, M., Chiang, C.-Y., Mitra, A.K., Zhang, Y., Curtis, M., Schryver, E.M., Bettis, S., et al. (2015). Quantitative high throughput screening using a primary human three-dimensional organotypic culture predicts in vivo efficacy. Nature Communications 6, 6220.

LaBarbera, D.V., Reid, B.G., and Yoo, B.H. (2012). The multicellular tumor spheroid model for high-throughput cancer drug discovery. Expert Opinion on Drug Discovery 7, 819-830.

Leight, J.L., Drain, A.P., and Weaver, V.M. (2017). Extracellular Matrix Remodeling and Stiffening Modulate Tumor Phenotype and Treatment Response. Annual Review of Cancer Biology 1, 313-334.

Long, G.V., Hauschild, A., Santinami, M., Atkinson, V., Mandalà, M., Chiarion-Sileni, V., Larkin, J., Nyakas, M., Dutriaux, C., Haydon, A., et al. (2017). Adjuvant Dabrafenib plus Trametinib in Stage III BRAF-Mutated Melanoma. New England Journal of Medicine 377, 1813-1823.

Macarron, R., Banks, M.N., Bojanic, D., Burns, D.J., Cirovic, D.A., Garyantes, T., Green, D.V.S., Hertzberg, R.P., Janzen, W.P., Paslay, J.W., et al. (2011). Impact of high-throughput screening in biomedical research. Nat Rev Drug Discov 10, 188-195.

Mathew, B., Schmitz, A., Muñoz-Descalzo, S., Ansari, N., Pampaloni, F., Stelzer, E.H.K., and Fischer, S.C. (2015). Robust and automated three-dimensional segmentation of densely packed cell nuclei in different biological specimens with Lines-of-Sight decomposition. BMC Bioinformatics 16, 187.

Mouw, J.K., Ou, G., and Weaver, V.M. (2014). Extracellular matrix assembly: a multiscale deconstruction. Nature Reviews Molecular Cell Biology 15, 771.

Packard, R.R.S., Baek, K.I., Beebe, T., Jen, N., Ding, Y., Shi, F., Fei, P., Kang, B.J., Chen, P.-H., Gau, J., et al. (2017). Automated Segmentation of Light-Sheet Fluorescent Imaging to Characterize Experimental Doxorubicin-Induced Cardiac Injury and Repair. Scientific Reports 7, 8603.

Paszek, M.J., Zahir, N., Johnson, K.R., Lakins, J.N., Rozenberg, G.I., Gefen, A., Reinhart-King, C.A., Margulies, S.S., Dembo, M., Boettiger, D., et al. (2005). Tensional homeostasis and the malignant phenotype. Cancer Cell 8, 241-254.

Santo, V.E., Rebelo, S.P., Estrada, M.F., Alves, P.M., Boghaert, E., and Brito, C. (2017). Drug screening in 3D in vitro tumor models: overcoming current pitfalls of efficacy read-outs. Biotechnology Journal 12, 1600505-n/a.

Shaffer, S.M., Dunagin, M.C., Torborg, S.R., Torre, E.A., Emert, B., Krepler, C., Beqiri, M., Sproesser, K., Brafford, P.A., Xiao, M., et al. (2017). Rare cell variability and drug-induced reprogramming as a mode of cancer drug resistance. Nature 546, 431-435.

Su, Y., Wei, W., Robert, L., Xue, M., Tsoi, J., Garcia-Diaz, A., Homet Moreno, B., Kim, J., Ng, R.H., Lee, J.W., et al. (2017). Single-cell analysis resolves the cell state transition and signaling dynamics associated with melanoma drug-induced resistance. Proceedings of the National Academy of Sciences of the United States of America 114, 13679-13684.

Theocharis, A.D., Skandalis, S.S., Gialeli, C., and Karamanos, N.K. (2016). Extracellular matrix structure. Advanced Drug Delivery Reviews 97, 4-27.

Tirosh, I., Izar, B., Prakadan, S.M., Wadsworth, M.H., Treacy, D., Trombetta, J.J., Rotem, A., Rodman, C., Lian, C., Murphy, G., et al. (2016). Dissecting the multicellular ecosystem of metastatic melanoma by single-cell RNA-seq. Science (New York, N.Y.) 352, 189-196.

Wells, R.G. (2008). The role of matrix stiffness in regulating cell behavior. Hepatology 47, 1394-1400.

Workman, P., Draetta, G.F., Schellens, J.H.M., and Bernards, R. (2017). How Much Longer Will We Put Up With $100,000 Cancer Drugs? Cell 168, 579-583.

Han, Y.L., Ronceray, P., Xu, G., Malandrino, A., Kamm, R.D., Lenz, M., Broedersz, C.P., and Guo, M. (2018). Cell contraction induces long-ranged stress stiffening in the extracellular matrix. Proceedings of the National Academy of Sciences.

Huisken, J., and Stainier, D.Y.R. (2007). Even fluorescence excitation by multidirectional selective plane illumination microscopy (mSPIM). Optics Letter 32, 2608-2610.

Welf, Erik S., Driscoll, Meghan K., Dean, Kevin M., Schäfer, C., Chu, J., Davidson, Michael W., Lin, Michael Z., Danuser, G., and Fiolka, R. (2016). Quantitative Multiscale Cell Imaging in Controlled 3D Microenvironments. Developmental Cell 36, 462-475.